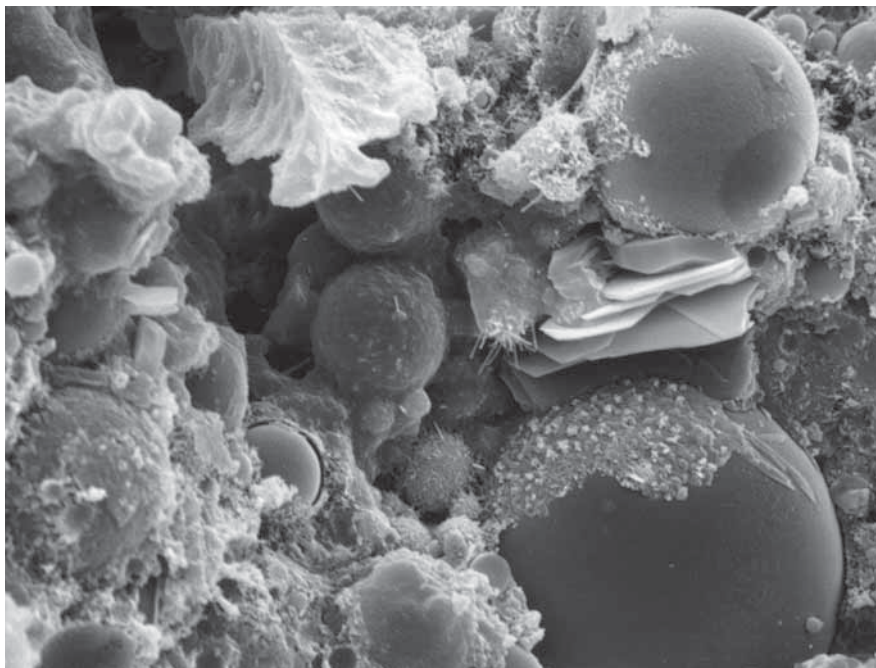


Materials, Systems and Structures in Civil Engineering 2016  
Segment on

## **Concrete with Supplementary Cementitious Materials**



Edited by  
Ole M. Jensen, Konstantin Kovler and Nele De Belie

**Proceedings  
PRO 113**



**International RILEM Conference on  
Materials, Systems and Structures in Civil Engineering 2016**

**segment on  
Concrete with Supplementary Cementitious Materials**

Published by RILEM Publications S.A.R.L.  
4 avenue du Recteur Poincaré 75016 Paris - France  
Tel : + 33 1 42 24 64 46 Fax : + 33 9 70 29 51 20  
<http://www.rilem.net> E-mail: [dg@rilem.net](mailto:dg@rilem.net)

© 2016 RILEM – Tous droits réservés.

ISBN: 978-2-35158-178-0 e-ISBN : 978-2-35158-179-7

Printed by Praxis – Nyt Teknisk Forlag, Ny Vestergade 17, 1471 København K, Denmark  
Photo 1<sup>st</sup> cover page: Fly ash particles embedded in different reaction products. Width of photo approximately 650 µm. Credit: Keren Binyamin & Konstantin Kovler (Technion)

**Publisher's note:** *this book has been produced from electronic files provided by the individual contributors. The publisher makes no representation, express or implied, with regard to the accuracy of the information contained in this book and cannot accept any legal responsibility or liability for any errors or omissions that may be made.*

*All titles published by RILEM Publications are under copyright protection; said copyrights being the property of their respective holders. All Rights Reserved.*

*No part of any book may be reproduced or transmitted in any form or by any means, graphic, electronic, or mechanical, including photocopying, recording, taping, or by any information storage or retrieval system, without the permission in writing from the publisher.*

RILEM, The International Union of Laboratories and Experts in Construction Materials, Systems and Structures, is a non profit-making, non-governmental technical association whose vocation is to contribute to progress in the construction sciences, techniques and industries, essentially by means of the communication it fosters between research and practice. RILEM's activity therefore aims at developing the knowledge of properties of materials and performance of structures, at defining the means for their assessment in laboratory and service conditions and at unifying measurement and testing methods used with this objective.

RILEM was founded in 1947, and has a membership of over 900 in some 70 countries. It forms an institutional framework for co-operation by experts to:

- optimise and harmonise test methods for measuring properties and performance of building and civil engineering materials and structures under laboratory and service environments,
- prepare technical recommendations for testing methods,
- prepare state-of-the-art reports to identify further research needs,
- collaborate with national or international associations in realising these objectives.

RILEM members include the leading building research and testing laboratories around the world, industrial research, manufacturing and contracting interests, as well as a significant number of individual members from industry and universities. RILEM's focus is on construction materials and their use in building and civil engineering structures, covering all phases of the building process from manufacture to use and recycling of materials.

RILEM meets these objectives through the work of its technical committees. Symposia, workshops and seminars are organised to facilitate the exchange of information and dissemination of knowledge. RILEM's primary output consists of technical recommendations. RILEM also publishes the journal *Materials and Structures* which provides a further avenue for reporting the work of its committees. Many other publications, in the form of reports, monographs, symposia and workshop proceedings are produced.

International RILEM Conference on Materials, Systems and Structures in Civil Engineering  
Conference segment on Concrete with Supplementary Cementitious Materials  
22-24 August 2016, Technical University of Denmark, Lyngby, Denmark

**International RILEM Conference on  
Materials, Systems and Structures in Civil Engineering 2016**

**Segment on  
Concrete with Supplementary Cementitious Materials**

Lyngby, Denmark

August 22-24, 2016

**Edited by  
Ole Mejlhede Jensen, Konstantin Kovler and Nele De Belie**

RILEM Publications S.A.R.L.

International RILEM Conference on Materials, Systems and Structures in Civil Engineering  
Conference segment on Concrete with Supplementary Cementitious Materials  
22-24 August 2016, Technical University of Denmark, Lyngby, Denmark

**Sponsors:**



**Knud Højgaards Foundation**

**Larsen & Nielsen foundation**

**Ingeborg og Leo Dannis Legat for Videnskabelig Forskning**

**Hosted by:**



**DANISH  
TECHNOLOGICAL  
INSTITUTE**

**International Organization by:**

- Nele De Belie (Ghent University, Belgium)
- Konstantin Kovler (Technion, Israel)
- Ole Mejlhede Jensen (Technical University of Denmark)

**Scientific Committee:**

Nele De Belie, Barbara Lothenbach, Josée Duchesne, Marios Soutsos, Konstantin Kovler, Guang Ye, John Provis, Carmen Andrade, Karen Scrivener, Mette Geiker, Wolfgang Brameshuber, Anya Vollpracht, Maria G. Juenger, Luc Courard, Jay G. Sanjayan, Duncan Herfort, Tongbo Sui, Jian Zhou, Ruben Snellings, Elke Gruyaert, Jeanette Visser, Geraldo Isaia, Harald Justnes, Toyoharu Nawa, Emmanuel Denarié, Jan Elsen, Yury Andrés Villagrán Zaccardi, R. Doug Hooton, Agnieszka J. Klemm, Antonios Kanellopoulos, Christos Dedeloudis, Manu Santhanam, Ahmed Loukili, Siham Kamali-Bernard, Fred Glasser, Angela Nunes, Winnie Matthes, Huan He, Luís Pedro Esteves, Esperanza Menéndez Méndez, Thomas Matschei, Eleni Arvaniti, Kosmas Sideris, Laurie Buffo-Lacarrière, Konstantin Sobolev, Susan A. Bernal, Cedric Patapy, Jose Fernando Martirena Hernández, Johann Plank.

## RILEM Publications

The following list presents the latest offer of RILEM Publications, sorted by series. Each publication is available in printed version and/or in online version.

### RILEM PROCEEDINGS (PRO)

**PRO 94 (online version):** HPFRCC-7 - 7th RILEM conference on High performance fiber reinforced cement composites, e-ISBN: 978-2-35158-146-9, *Eds. H.W. Reinhardt, G.J. Parra-Montesinos, H. Garrecht*

**PRO 95:** International RILEM Conference on Application of superabsorbent polymers and other new admixtures in concrete construction, ISBN: 978-2-35158-147-6; e-ISBN: 978-2-35158-148-3, *Eds. Viktor Mechtcherine, Christof Schroefl*

**PRO 96 (online version):** XIII DBMC: XIII International Conference on Durability of Building Materials and Components, e-ISBN: 978-2-35158-149-0, *Eds. M. Quattrone, V.M. John*

**PRO 97:** SHCC3 – 3rd International RILEM Conference on Strain Hardening Cementitious Composites, ISBN: 978-2-35158-150-6; e-ISBN: 978-2-35158-151-3, *Eds. E. Schlangen, M.G. Sierra Beltran, M. Lukovic, G. Ye*

**PRO 98:** FERRO-11 – 11th International Symposium on Ferrocement and 3rd ICTRC - International Conference on Textile Reinforced Concrete, ISBN: 978-2-35158-152-0; e-ISBN: 978-2-35158-153-7, *Ed. W. Brameshuber*

**PRO 99 (online version):** ICBBM 2015 - 1st International Conference on Bio-Based Building Materials, e-ISBN: 978-2-35158-154-4, *Eds. S. Amziane, M. Sonebi*

**PRO 100:** SCC16 - RILEM Self-Consolidating Concrete Conference, ISBN: 978-2-35158-156-8; e-ISBN: 978-2-35158-157-5

**PRO 101 (online version):** III Progress of Recycling in the Built Environment, e-ISBN: 978-2-35158-158-2, *Eds I. Martins, C. Ulsen and S. C. Angulo*

**PRO 102 (online version):** RILEM Conference on Microorganisms-Cementitious Materials Interactions, e-ISBN: 978-2-35158-160-5, *Eds. Alexandra Bertron, Henk Jonkers, Virginie Wiktor*

In relation to the International RILEM Conference on Materials, Systems and Structures in Civil Engineering, MSSCE 2016 which the present proceedings belongs to, the following RILEM proceedings will be issued:

**PRO 108:** Innovation of Teaching in Materials and Structures

**PRO 109** (two volumes): Service life of Cement-Based Materials and Structures

**PRO 110:** Historical Masonry

**PRO 111:** Electrochemistry in Civil Engineering

**PRO 112:** Moisture in Materials and Structures

**PRO 113:** Concrete with Supplementary Cementitious materials

**PRO 114:** Frost Action in Concrete

**PRO 155:** Fresh Concrete

### RILEM REPORTS (REP)

**Report 45:** Repair Mortars for Historic Masonry - State-of-the-Art Report of RILEM Technical Committee TC 203-RHM, e-ISBN: 978-2-35158-163-6, *Ed. Paul Maurenbrecher and Caspar Groot*



## Contents

	<i>Page</i>
<b>Preface</b>	XI
Ole Mejlhede Jensen, Konstantin Kovler, Nele De Belie	
<b>Welcome</b>	XII
Ole Mejlhede Jensen	
1. <b>Performance evaluation of Aplite rock based geo-polymer binder</b>	1
Samindi Samarakoon, Samdar Kakay, Erland Soli Johnsen, Fredrik Meidell Knutsen, Jon Emil Tobias Knutsson	
2. <b>Evaluation of hardened state properties of GGBS-PC mortars modified by superabsorbent polymers (SAP)</b>	11
Fernando C. R. Almeida, Agnieszka J. Klemm	
3. <b>Can superabsorbent polymers mitigate shrinkage in cementitious materials blended with supplementary cementitious materials?</b>	21
Didier Snoeck, Ole Mejlhede Jensen, Nele De Belie	
4. <b>Influence of particle size distribution of slag, limestone and fly ash on early hydration of cement assessed by isothermal calorimetry</b>	31
Yury Villagrán Zaccardi, Elke Gruyaert, Natalia Alderete, Nele De Belie	
5. <b>Reactivity of fly ash in the presence of chemical activators</b>	41
Frank Winnefeld, Salaheddine Alahrache, Jean-Baptiste Champenois, Frank Hesselbarth, Barbara Lothenbach	
6. <b>Comparison of reaction degrees of slag and fly ash obtained by thermogravimetry and selective dissolution</b>	51
Yury Villagrán Zaccardi, Elke Gruyaert, Nele De Belie	
7. <b>Particle Size Distribution and Specific Surface Area of SCMs compared through experimental techniques</b>	61
Natalia M. Alderete, Yury A. Villagrán, Gabriela S. Coelho Dos Santos, Nele De Belie	
8. <b>Effect of SCMs on hydration kinetics of Portland cements</b>	73
Barbara Lothenbach, Axel Schöler, Maciej Zajac, Mohsen Ben Haha, Frank Winnefeld	
9. <b>Effect of fly ash on pore structure of hardened cement paste measured by thermoporometry</b>	83
Kiyofumi Kurumisawa, Takuya Sugiyama, Masanori Miyamoto, Toyoharu Nawa	
10. <b>Radiological study of cements and geopolymers</b>	93
Francisca Puertas, Catalina Gasco, Luis Yague, Nuria Navarro, José Antonio Suarez, Mar Alonso, Manuel Torres, Patricia Rivilla	
11. <b>Supplementary cementitious materials in the era of sustainable concrete</b>	103
Vyacheslav Falikman, Nikolai Bashlykov	
12. <b>Realizing the strengths of SCM concretes by recognizing its weaknesses</b>	113
R. Doug Hooton	
13. <b>Durability of high volume fly ash concrete</b>	123
Himabindu Myadaraboina, Mochamad Solikin, Indubhushan Patnaikuni	



14. <b>Natural Zeolites as SCMs: Challenges and solutions</b>	133
Maria Juenger, Lisa Burris, Saamiya Seraj, Raissa Ferron	
15. <b>Effects of w/p ratio and limestone filler on permeability of cement pastes</b>	141
Quoc Tri Phung, Norbert Maes, Diederik Jacques, Geert De Schutter, Guang Ye	
16. <b>Predictions of the mechanical performance of concrete made with ternary cements</b>	153
Kim-Séang Lauch, Vinciane Dieryck, Benoit Parmentier	
17. <b>Durability of concrete made with ternary cements containing slag or fly ash and limestone filler</b>	165
Kim-Séang Lauch, Vinciane Dieryck	
18. <b>Comparison of the expansion of mortar containing shell powder of surf clam and scallop</b>	177
Akio Watanabe, Kazumi Hirokawa, Takashi Kondo	
19. <b>Eco-concrete for precast elements with effective mineral micro- and eco-fillers</b>	189
Gheorghe-Alexandru David, Joachim Juhart, Elke Krischey, Claudia Baldermann, Florian Mittermayr, Markus Krüger	
20. <b>The effect of SCM replacement on autogenous deformation of high performance concrete</b>	199
Abdulaziz Alaskar, R. Douglas Hooton	
21. <b>Calcined dredged sediments as supplementary cementitious materials: properties and pozzolanic reactivity</b>	205
Ruben Snellings, Liesbeth Horckmans, Pawel Durdzinski, Céline Van Bunderen, Lucie Vandewalle, Koenraad Van Balen, Joris Dockx, Jos Vandekeybus, Özlem Cizer	
22. <b>High volume fly ash hybrid alkali activated cements and concretes for indoor application</b>	213
Pavel Krivenko, Oleksandr Kovalchuk, Valentina Grabovchuk	
23. <b>Physical and mechanical properties of cement mortars with biomass ashes as SCM</b>	223
Mirjana Malešev, Vlastimir Radonjanin, Miroslava Radeka, Slobodan Šupić, Suzana Draganić	
24. <b>Differentiating the physical and chemical effects of supplementary cementitious materials in cement mortars</b>	233
Manu Santhanam, Hemalatha M S	
25. <b>Coal bottom ash feasibility study to be a new Portland cement constituent</b>	243
Miguel Angel Sanjuán, Esperanza Menéndez, Cristina Argiz, Amparo Moragues	
26. <b>Physical properties and pore solution analysis of alkali activated fly ash-slag pastes</b>	253
Marija Nedeljković, Yibing Zuo, Kamel Arbi, Guang Ye	
27. <b>Carbonation mechanism of different kinds of C-S-H: Rate and products</b>	263
Bei Wu, Guang Ye	
28. <b>Investigation of the moisture influence on permeation properties of alkali-activated slag concrete</b>	273
Kai Yang, Sreejith Nanukuttan, Changhui Yang, Bryan Magee, Jianxiong Ye, Muhammed Basheer	

29. <b>The rate of strength development of mortar mixes with SCMs at elevated curing temperatures</b>	283
Marios Soutsos, Gidion Turu'allo	
30. <b>Outcomes of the RILEM round robin on degree of reaction of slag and fly ash in composite cements</b>	293
Paweł T. Durdziński, Mohsen Ben Haha, Susan A. Bernal, Nele De Belie, Elke Gruyaert, Barbara Lothenbach, John L. Provis, Axel Schöler, Christopher Stabler, Zhijun Tan, Anya Vollpracht, Frank Winnefeld, Yury Villagrán Zaccardi, Maciej Zajac, Karen L. Scrivener	
31. <b>Effect of testing conditions on the loss on ignition results of anhydrous granulated blast furnace slags determined via thermogravimetry</b>	299
Susan Bernal, Xinyuan Ke, Oday Hussein, John Provis	
32. <b>Influence of SCM on pore solution composition</b>	309
Anya Vollpracht, Barbara Lothenbach, Ruben Snellings, Johannes Haufe	
33. <b>Chloride penetration in concrete under compression or splitting tensile load representing 60 - 65 per cent of the ultimate load</b>	319
Hugo Eguez, Nele De Belie, Geert De Schutter	
34. <b>Applicability of Nordic clays as SCM</b>	331
Harald Justnes, Tone Østnor, Serina Ng	
35. <b>Production of ceramics using bottom ash and fly ash from a thermal power plant</b>	341
Biljana Angjusheva, Emilija Fidancevska, Vilma Ducman, Ljubica Vladicevska	
36. <b>Ultra high performance concrete (UHPC) with low silica fume contents and limestone aggregates</b>	349
Guillermo Hernández-Carrillo, Alejandro Durán-Herrera, Pedro L. Valdez-Tamez	
37. <b>Internal curing of high performance concrete with superabsorbent polymers: Evaluation of durability</b>	359
Jennifer Anette Canul Polanco, Alejandro Durán Herrera, Pedro Leobardo Valdez Tamez	
38. <b>Do supplementary cementitious materials and blended cements indeed increase cracking potential of concrete?</b>	371
Konstantin Kovler	
39. <b>Replacement of cement with waste ceramic powder in cementitious composites: Results of a preliminary investigation</b>	383
Liberato Ferrara, Peter Deegan, Andrea Pattarini, Mohammed Sonebi, Su Taylor	
40. <b>Permeability of ambient cured fly ash geopolymer concrete blended with additives</b>	393
Pradip Nath, Prabir Sarker	
41. <b>Sintering of ceramics based on mechanically activated fly ash</b>	403
Emilija Fidanchevski, Jorg Bossert, Biljana Angjusheva, Vojo Jovanov, Vineta Srebrenkoska	
42. <b>Investigation of the effect of partial replacement of Portland cement by fly ash on carbonation using TGA and SEM-EDS</b>	413
Andres Belda Revert, Klaartje De Weerd, Karla Hornbostel, Mette Geiker	

43. <b>Effects of waste glass and activating solution on tungsten mining waste alkali-activated binders</b>	423
Gediminas Kastiukas, Xiangming Zhou	
44. <b>Performance of alusilica as mineral admixture in cementitious systems</b>	433
Lin Chi, Ole Mejlhede Jensen	
45. <b>Mitigation of early age shrinkage in self-consolidating paste systems using superabsorbent polymers</b>	443
Syed Ali Rizwan, Shozab Mustafa, Waleed Ahmed	
<b>Author Index</b>	455

## **SINTERING OF CERAMICS BASED ON MECHANICALLY ACTIVATED FLY ASH**

**Emilija Fidanchevski<sup>(1)</sup>, Jörg Bossert<sup>(2)</sup>, Biljana Angjusheva<sup>(1)</sup>, Vojo Jovanov<sup>(1)</sup>, Vineta Srebrenkoska<sup>(3)</sup>**

(1) Ss Cyril and Methodius University in Skopje, Macedonia

(2) Friedrich-Schiller-Universität Jena, Germany

(3) Goce Delcev University, Shtip, Macedonia

### **Abstract**

This paper presents the results for the influence of the mechanical activation on the properties of the sintered fly ash compacts. By varying the time of mechanical activation (short time of 10, 20 and 30 min) and temperature of sintering: 1050, 1100 and 1130 °C/60 min a spectrum of properties was obtained, but as an optimal defined was the mechanical activation of 20 min prior to the sintering at 1130°C.

### **1. Introduction**

Solid waste (fly ash and bottom ash) generated from the thermal power plant during the combustion of coal to produce electricity presents the global problem from the environmental point of view. Part of the generated fly ash is successfully used in the cements production [1], but also the possibilities to incorporate fly ash into ceramics matrices like in tiles [2] and bricks [3], in the production of mullite [4] as well as in geopolymers [5] are widely reported. Fly ash presents valuable low cost material due to its chemical composition consisting mainly of SiO<sub>2</sub>, Al<sub>2</sub>O<sub>3</sub>, CaO, Fe<sub>2</sub>O<sub>3</sub>. Physical properties of fly ash depend on the burning conditions and the type of coal. The shape of the fly ash particles are mostly spherical with specific surface area from 250 to 600m<sup>2</sup>/kg. As far as it is very fine material it is usually used as raw material with no pre-treatment [6, 7]. By increasing the geometrical factor of activity – specific surface area and reducing the particle size distribution the consolidation of the powder is favored, usually at lower temperatures.

This paper presents the results obtained from the investigation realized by pre-treating the fly ash i.e. thermal treatment (600°C) and mechanical activation for short period of time (10, 20 and 30 min). Also, the influence of the pretreatment on the final properties and the microstructure is discussed.

## 2. Materials and methods

Fly ash used in this investigation was obtained from the thermal power plant REK Bitola, Republic of Macedonia, derived from lignite combustion. X-Ray Fluorescence (model ARL 990XP) was used for determination of the chemical composition of fly ash. The loss of ignition (LOI) was determined by calcination of pre-dried samples at 900<sup>0</sup>C/2h. Residual coal contained in the ashes was determined from the mass loss after 2 hours at 600<sup>0</sup>C. Particle size distribution of the fly ash was determined by sieving analyses (Retsch AS200) and the specific gravity was calculated using the pycnometer method.

The morphology of the fly ashes during the investigation was followed by scanning electron microscopy (Leica S 440I) coupled with EDS, which was used for determination of chemical composition of particular fly ash particles.

The thermal properties of the pressureless prepared fly ashes compacts were determined using a heating microscope (Leitz Wetzlar) in the temperature interval of RT-1400<sup>0</sup>C, in air atmosphere with a heating rate of 10 <sup>0</sup>C/min. Dilatometry (NETZSCH 402E) was used to follow the shrinkage of the pressed fly ash samples during sintering from RT to 1130<sup>0</sup>C.

In order to increase the structural and geometrical activity of the fly ash, mechanical activation was applied in vibro mill. Mechanical activation was applied for a short time (period of 10, 20 and 30 min) in order to follow the obtained properties on the sintered fly ash compacts. The fly ash samples in this investigation were assigned as: TFA for thermally treated fly ash at 600<sup>0</sup>C, and TFA-MA10, TFA-MA20 and TFA-MA30 for the fly ash samples thermally treated and mechanically activated for 10, 20 and 30 min prior to the sintering.

Fly ashes were consolidated by uniaxial pressing ( $P = 45$  MPa) using 8% water as a binder. The compacted green samples were dried at 105<sup>0</sup>C for 10 hours prior to the sintering. The sintering of the TFA samples was realized at 1050, 1100, 1150 and 1200<sup>0</sup>C, but for the mechanically activated fly ashes (TFA-MA10, TFA-MA20 and TFA-MA30), the sintering was realized at three different temperatures: 1050, 1100 and 1130<sup>0</sup>C using chamber furnace. The applying heating rate was 10<sup>0</sup>C/min. The isothermal treatment at final temperature was 60 min. The cooling to RT was not controlled.

Water displacement method according to EN-993 was used for determination the bulk density. Porosity was calculated from the relative density.

The bending strength and E-modulus of the sintered fly ash compacts were determined with the 3-point bending strength tester (Netzsch 401/3) with 30mm span and 0.5mm/min loading rate. Instron testing machine (model 1126) with a crosshead speed of 0.5 mm/min was used for the compressive strength test. Three samples were used for determination of the mechanical properties and the average values were reported as the result.

### 3. Results and discussion

The chemical composition of the investigated fly ash is presented in the Table 1. According to the CaO which is 11.49wt.% this fly ash can be classified as C class fly ash according to the ASTM C618 definitions. The free CaO was not detected. Residual (unburned) coal contained in the fly ash was 2.75 wt.% .

Table 1: Chemical composition of fly ash

Oxide	SiO <sub>2</sub>	Al <sub>2</sub> O <sub>3</sub>	Fe <sub>2</sub> O <sub>3</sub>	CaO	MgO	K <sub>2</sub> O	Na <sub>2</sub> O	SO <sub>3</sub>	LOI
wt.%	54.74	20.29	6.76	11.49	2.46	1.57	0.93	0.93	3.12

It is evident from the chemical composition presented in Table 1 that silica (SiO<sub>2</sub>) and alumina (Al<sub>2</sub>O<sub>3</sub>) are the main oxides, but besides them, fly ash has a significant amount of calcium oxide (CaO) and iron oxide (as ferric). The integral content of SiO<sub>2</sub> comes from SiO<sub>2</sub> - quartz, CaAl<sub>2</sub>Si<sub>2</sub>O<sub>8</sub> – anorthite and NaAlSi<sub>3</sub>O<sub>8</sub> – albite and according to the XRD the presence of Fe<sub>2</sub>O<sub>3</sub> - hematite, CaSO<sub>4</sub> - anhydrite and an amorphous phase was also determined [8].

Fly ash belongs to the relatively fine materials and according to the granulometric composition, Table 2, almost 50% of fly ash particles are less than 63µm. The specific gravity of the fly ash is 2.17g/cm<sup>3</sup>.

Table 2: Granulometric composition of as received fly ash

Diameter, (mm)	Fly ash, (wt.%)
+1.0	0.6
-1.0+0.5	1.5
-0.5+0.25	7.6
-0.25+0.125	18.0
-0.125+0.063	25.2
-0.063	47.1
<b>Σ</b>	100

The morphology of fly ash is presented in Figure 1. Figures 2-4 and Table 3 present the morphology and the chemical composition (microprobe analysis) of the Fe<sub>2</sub>O<sub>3</sub>, needle SiO<sub>2</sub> and amorphous silica (diatomite). Typical fly ash cenospheres are presented in Figure 3 and the rough surface particle presents hematite.

In the present investigation, in order to reduce the sintering temperature of fly ash, mechanical activation during short period of time (10, 20 and 30 min) was performed. Morphology of the

TFA particles and after mechanical activation (TFA-MA10, TFA-MA20 and TFA-MA30) are presented in Figures 5-8. It is evident that by increasing the time of mechanical activation the particles reduced their dimension. After 10 min of milling, part of the particles remain their start dimensions, but the biggest part of the particles changed their dimension and morphology. The dimension of the particles, TFA-MA10, varied from 2 to 50 $\mu\text{m}$ , but for the TFA-MA20 and TFA-MA30 the particles sized distribution varied from 1 to 30  $\mu\text{m}$  and 1 to 20 $\mu\text{m}$ , respectively.

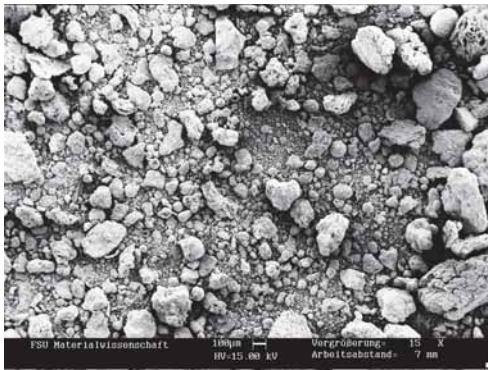


Figure 1. Morphology of fly ash (bar 1 $\mu\text{m}$ )

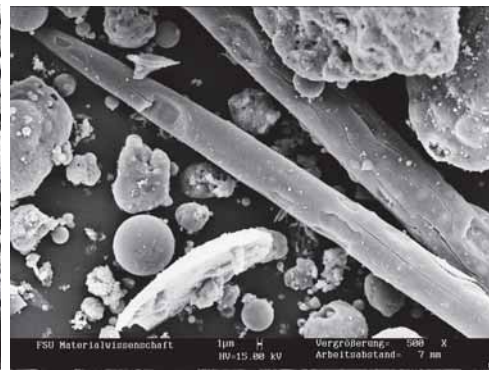


Figure 2. Morphology of needle SiO<sub>2</sub> (bar 1 $\mu\text{m}$ )



Figure 3. Morphology of Fe<sub>2</sub>O<sub>3</sub> (bar 1 $\mu\text{m}$ )

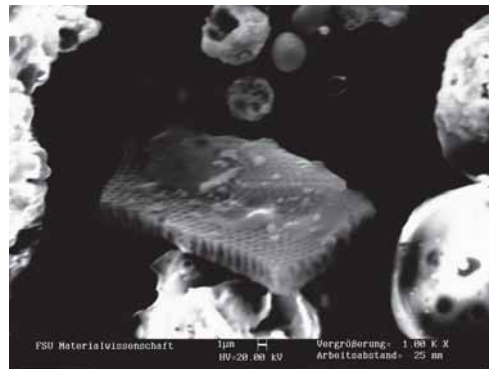


Figure 4. Morphology of diatomite (bar 1 $\mu\text{m}$ )

The thermal characteristics of pressure less prepared fly ash samples before (TFA) and after mechanical activation (TFA-MA10, TFA-MA20 and TFA-MA30) are presented in Table 4.



Table 3: Chemical composition of the particular fly ash particles – needle quartz, hematite and diatomite

Oxide	Needle quartz, (wt.%)	Hematite sphere, (wt.%)	Diatomite, (wt.%)
SiO <sub>2</sub>	98.12	1.75	95.48
Al <sub>2</sub> O <sub>3</sub>	0.56	0.13	1.62
Fe <sub>2</sub> O <sub>3</sub>	0.35	97.07	-
CaO	0.22	0.35	0.37
MgO	0.18	0.13	0.01
K <sub>2</sub> O	0.06	0.11	0.20
Na <sub>2</sub> O	0.33	0.07	0.70
SO <sub>3</sub>	0.09	0.02	0.53
TiO <sub>2</sub>	0.05	0.15	0.04
MnO	0.01	0.05	0.02
Cr <sub>2</sub> O <sub>3</sub>	0.04	0.08	0.50

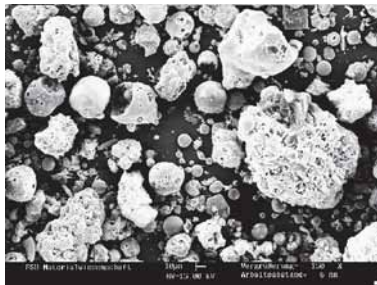


Figure 5. Morphology of TFA (bar 10µm)



Figure 6. Morphology of TFA-MA10 (bar 10µm)

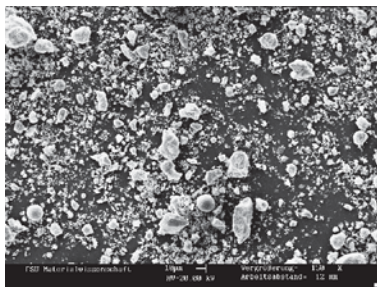


Figure 7. Morphology of TFA-MA20 (bar 10µm)

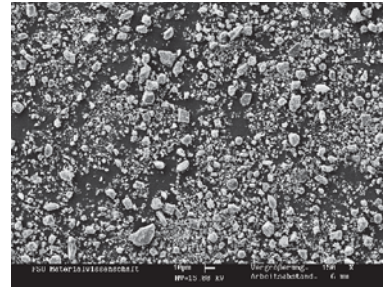


Figure 8. Morphology of TFA-MA30 (bar 10µm)



Table 4: Thermal characteristics of fly ash before (TFA) and after different time of mechanical activation (TFA-MA10, TFA-MA20 and TFA-MA30)

Type of fly ash	Significant shrinkage, $^{\circ}\text{C}$	Softening temperature, $^{\circ}\text{C}$	Melting temperature, $^{\circ}\text{C}$
TFA	1220±10	1260±10	1360±10
TFA-MA10	1160±10	1220±10	1350±10
TFA-MA20	1150±10	1210±10	1340±10
TFA-MA30	1145±10	1215±10	1345±10

The region of sintering of fly ash before mechanical activation, TFA, is 1220 - 1260±10<sup>0</sup>C, but it is reduced with the increase of the time of mechanical activation. The sintering regions for the mechanically activated fly ashes are: 1160 - 1220 ±10<sup>0</sup>C for TFA-MA10, 1150 - 1210±10<sup>0</sup>C for TFA-MA20 and 1145 - 1215±10 for TFA-MA30. The particle size of fly ash decreased during the mechanical activation and this results in the decrease of the melting temperature from 1360±10<sup>0</sup>C for the starting fly ash (TFA) to 1345±10<sup>0</sup>C for fly ash mechanically activated for 30 min (TFA-MA30).

After the consolidation of the fly ash powders by pressing, the shrinkage of the consolidated samples during sintering was followed by dilatometry. The dependances of the shrinkage with temperature in the polythermal part of sintering for the fly ash before (TFA) and after mechanical activation (TFA-MA10, TFA-MA20 and TFA-MA30) are presented in Figure 9. The shrinkage of TFA started at 400<sup>0</sup>C and continues slightly up to 1100<sup>0</sup>C, reaching the total shrinkage of 2.61mm at 1130<sup>0</sup>C. The shrinkage for mechanically activated fly ash samples (TFA-MA10, TFA-MA20 and TFA-MA30) starts at a temperature 730<sup>0</sup>C and up to the temperature of 1050<sup>0</sup>C it showed slight shrinkage followed by rapid shrinkage up to the temperature of 1130<sup>0</sup>C. Mechanically activated TFA-MA20 sample showed maximal shrinkage of 4.72mm.

Sintered fly ash compacts were characterized from physical (density and porosity) and mechanical (bending strength, E-modulus and compressive strength) aspect. The properties of the sintered fly ash compacts are presented in Table 5.

Generally, by increasing the sintering temperature and the time of mechanical activation the density and mechanical properties increased, but the porosity decreased for the all sintered fly ash samples (TFA, TFA-MA10 TFA-MA20 and TFA-MA30).

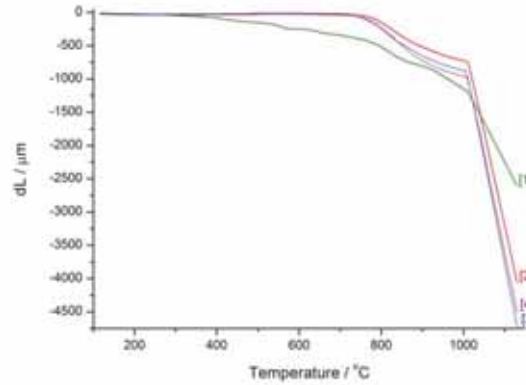


Figure 9. Shrinkage /temperature dependence in polythermal part of sintering for: TFA, curve [1]; TFA-MA10, curve [2]; TFA-MA20, curve [3] and TFA-MA30, curve [4].

Table 5: Physical and mechanical properties of sintered TFA, TFA-MA10 TFA-MA20 and TFA-MA30 samples

Sample	T, °C	Density, g/cm <sup>3</sup>	Porosity, %	E-modulus, GPa	Bending strength, MPa	Compressive strength, GPa
TFA	1050	1.25	47.01	2.17	1.71	2.49
	1100	1.29	46.89	1.88	2.67	2.55
	1150	1.46	44.07	6.73	7.27	8.32
	1200	2.01	1.66	21.34	35.47	32.30
TFA-MA10	1050	1.60	40.69	6.54	11.44	19.47
	1100	1.62	38.98	8.16	17.32	27.84
	1130	2.27	15.37	41.17	74.30	67.67
TFA-MA20	1050	1.61	39.98	7.13	11.95	19.65
	1100	1.63	37.64	9.94	18.51	31.53
	1130	2.34	11.46	48.04	79.90	78.48
TFA-MA30	1050	1.62	39.14	7.26	12.42	22.91
	1100	1.65	37.12	11.73	21.75	35.65
	1130	2.45	9.89	50.65	83.58	80.54

TFA compacts have low values for mechanical properties (up to 8.32 GPa compressive strength for the sample sintered at 1150<sup>0</sup>C) except the compacts sintered at 1200<sup>0</sup>C. The values for mechanical properties are almost 3 to 4 times higher as the sintering temperature

increased from 1150 to 1200°C. The comparable microstructures for the sintered TFA compacts at 1150 and 1200°C are presented in Figures 10 and 11. The effect of the different degree of sintering is evident. At temperature of 1150°C, part of the fly ash particles lost their individuality and the appearance of the liquid phase among the spherical fly ash particles is evident. Liquid phase sintering is favoured at 1200°C.

The presented results for the mechanically activated fly ashes (TFA-MA10, TFA-MA20 and TFA-MA30), Table 5, showed that the properties increased significantly after 10 min of mechanical activation (in comparison to TFA) and there are no significant changes of the properties for 20 and 30 min of mechanical activation (TFA-MA20 and TFA-MA30). The values of density, porosity and mechanical properties have no significant differences for all fly ash compacts sintered at 1050 and 1100°C, but the rapid changes of the values occurs for the fly ash compacts sintered at 1130°C. The microstructures of the fly ash compacts (TFA-MA10, TFA-MA20 and TFA-MA30) sintered at maximal temperature of 1130°C are presented in Figures 12 - 14.



Figure 10. Microstructure of TFA compacts sintered at 1150°C (bar: 2µm)

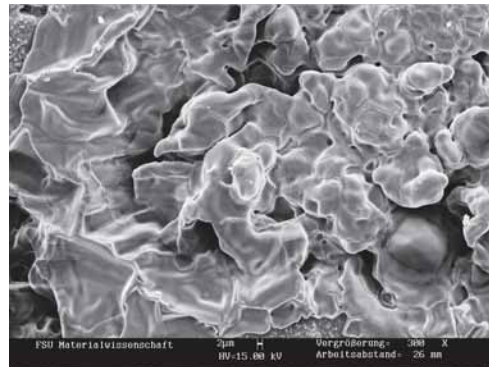


Figure 11. Microstructure of TFA sintered at 1200°C (bar: 2µm)

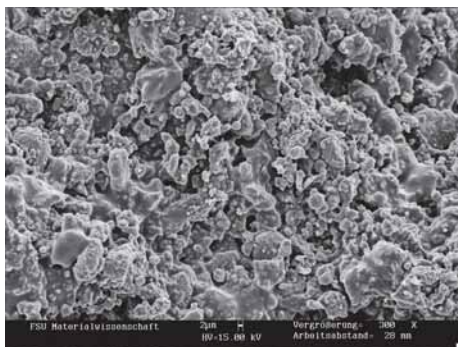


Figure 12. Microstructure of TFA-MA10 sintered at 1130°C/1h, (bar 2 µm)

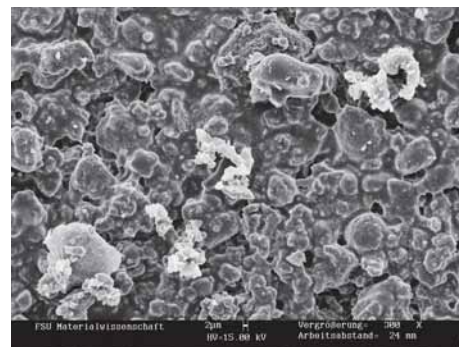


Figure 13. Microstructure of TFA-MA20 sintered at 1130°C/1h, (bar 2 µm)



Figure 14. Microstructure of TFA-MA30 sintered at 1130°C/1h, (bar 2 µm)

Intragranular pores with dimensions from 3 to 8 µm are present in the microstructure of the TFA-10 compact (Figure 12) and also local appearance of liquid phase is evident. The bigger quantity of liquid phase is typical for the TFA-MA20 (Figure 13) where the biggest part of the grains are covered with the liquid phase. The pores with dimensions from 4 to 8 µm are present between particular grains and non-coherent layer of the liquid phase. By increasing the time of mechanical activation to 30 min, sample TFA-MA30, the coherent part of liquids phase (Figure 13) transforms to inherent layer (Figure 14). The dimensions of the grains are from 3 to 50 µm.

#### 4. Conclusion

In this investigation by varying the process parameters (short time of mechanical activation: 10, 20 and 30 min and sintering temperatures: 1050, 1100 and 1130°C) a spectrum of properties is achieved. The defined optimal conditions in this investigation were a sintering temperature of 1130°C and 20 min of mechanical activation prior to the sintering.

The obtained fly ash compacts pre-treated at 600°C and mechanically activated for 20 min prior to the sintering at 1130°C has the following properties: density: 2.34g/cm<sup>3</sup>; porosity:11.46%; E-modulus: 48.04 GPa; bending strength: 79.90 MPa and compressive strength - 78.48 GPa. The compacts can be potentially used for construction purposes.

#### Acknowledgement

The financial support from DAAD, Germany is gratefully acknowledged and also to COST Action TU1301. [www.norm4building.org](http://www.norm4building.org).

## References

- [1] Ng, S. and Justnes, H., Influence of plasticizers on the rheology and early heat of hydration of blended cements with high content of fly ash, *Cement Concrete Comp* 65 (2016), 41-45
- [2] Sokolar, R. and Smetanova, L., Dry pressed ceramic tiles based on fly ash–clay body: Influence of fly ash granulometry and pentasodium triphosphate addition, *Ceram Int* 36 (2010), 215-221
- [3] Çiçek, T. and Çinçin, Y., Use of fly ash in production of light-weight building bricks, *Constr Build Mater* 94 (2015), 521-527
- [4] Lin, B., Li, S., Hou, X., Li, H., Preparation of high performance millite ceramics from high-aluminum fly ash by an effective method, *J Alloy Compd* 623 (2015), 359-361
- [5] Papias, D., Giannopoulou, I.P., Perraki, T., Effect of synthesis parameters on the mechanical properties of fly ash-based geopolymers, *Colloid Surface A* 301 (2007), 246-254
- [6] Biernacki, J.J., Vazrala, A.K., Leimer, H.W., Sintering of a class F fly ash, *Fuel* 87, (2008), 782-792
- [7] Erol, M., Küçükbayrak, S., Ersoy-Meriçboyu, A., Characterization of sintered coal fly ashes, *Fuel* 87 (2008), 1334-1340
- [8] Angusheva, B., Fidancevska, E., Jovanov, V., Production of ceramics based on fly ash, *Chem Ind Chem Eng Q* 18 (2012), 245-254